KKU Engineering Journal

http://www.en.kku.ac.th/enjournal/th/

Laminar periodic flow and heat transfer in square duct with 30° end-trimmed rectangular winglet

Amnart Boonloi[1)], Withada Jedsadaratanachai[2)]*, Pongjet Promvonge[2)]

[1)]Department of Mechanical Engineering Technology, College of Industrial Technology,
King Mongkut's University of Technology North Bangkok, Bangkok, Thailand, 10800

[2)]Department of Mechanical Engineering, Faculty of Engineering,
King Mongkut's Institute of Technology Ladkrabang, Bangkok, Thailand, 10520

Received June 2012
Accepted February 2013

Abstract

A numerical investigation has been carried out to examine laminar flow and heat transfer characteristics in a three-dimensional isothermal wall duct with 30° end-trimmed rectangular winglet. The computations are based on the finite volume method, and the SIMPLE algorithm has been implemented. The fluid flow and heat transfer characteristics are presented for Reynolds numbers based on the hydraulic diameter of the duct ranging from 100 to 2000. To generate vortex flows through the square duct, winglet with an attack angle of 30° are mounted in the square duct. Effects of different flow blockage areas with single pitch length ratios on heat transfer and friction loss are investigated. It is apparent that the main vortex flows created by the 30° end-trimmed rectangular winglet exist and help to induce impinging flows on the wall of the winglet cavity leading to drastic increase in heat transfer rate over the duct. In addition, the rise in the winglet height results in the increase in the friction factor values. The computational results reveal that the maximum thermal enhancement factors for the end-trimmed with *BR*=0.10 is found to be about 4.10 at *Re*=2000.

Keywords : Periodic flow, Square duct, Laminar flow, Heat transfer, Rectangular winglet

*Corresponding author. Tel.: +66-2329-8350; fax: +66-2329-8352
Email address: kjwithad@kmitl.ac.th

1. Introduction

The application of ribs/baffles/winglets mounted in the cooling/heating ducts or heat exchanger tubes is one of the commonly used passive heat transfer enhancement technique in single-phase internal flows since periodically positioned ribs in the ducts interrupt hydrodynamic and thermal boundary layers, apart from inducing recirculation flow. Downstream of each rib/baffle the flow separates, recirculates, and impinges on the duct wall and these effects are the vital reasons for heat transfer enhancement in such ducts. The use of ribs/baffles/winglets [1-3] increases not only the heat transfer rate but also substantial the pressure loss. It is, thus, difficult to realize the advantage of rib/baffle arrangements and the staggered rib/baffle with its pitch spacing of 1 time the duct height is often recommended in most of previous work.

The first work on the numerical investigation of flow and heat transfer characteristics in a duct with the concept of periodically fully developed flow was conducted by Patankar *et al.* [4] and since then, periodic duct flows for laminar and turbulent regimes have been applied extensively. Berner *et al.* [5] suggested that a laminar behavior for a channel with transverse baffles mounted on two opposite walls is found at a Reynolds number below 600 and for such conditions the flow is free of vortex shedding. Lopez *et al.* [6] carried out a numerical investigation on laminar forced convection in a three-dimensional channel with baffles for periodically fully developed flow and with a uniform heat flux in the top and bottom walls. Promvonge *et al.* [7] studied numerically the laminar heat transfer enhancement in a square channel with 45° inclined baffle on one wall and a single baffle pitch. They found that a single streamwise vortex flow is created by the baffle throughout the channel and a vortex flow exists and helps to induce impingement jets on the upper, lower and baffle trailing end (*BTE*) side walls. The appearance of vortex–induced impingement (*VI*) flows leaded to the maximum thermal enhancement factor of about 2.2 at *BR*=0.4 and *Re*=1200. Promvonge *et al.* [8] also investigated numerically the laminar flow structure and thermal behaviors in a square channel ith 45° inline baffles on two opposite walls. Two streamwise counter-rotating vortex flows were created along the channel and *VI* jets appeared on the upper, lower and baffle leading end (*BLE*) side walls. The maximum thermal enhancement factors of about 2.6 at *BR*=0.2, *PR*=1 and *Re*=1000 were reported, respectively. A numerical investigation of Murata and Mochizuki [9] on heat transfer characteristics in a ribbed square duct with *e*/*D*=0.1, *P*/*e*=10 and 60° orientation using a large eddy simulation provided that the flow reattachment at the midpoint between ribs caused a significant increase in the local heat transfer.

Most of the investigations, cited above, have considered the heat transfer characteristics for transverse ribs/baffles placed repeatedly in square/rectangular channels only. The application of end-trimmed rectangulat winglet attached in square duct walls has rarely been reported. In the present work, the numerical computations for three dimensional laminar periodic square flows over the 30° end-trimmed rectangulat winglet mounted periodically on the duct wall with in-line arrangement and pointing upstream are conducted with the main aim being to examine the changes in the flow structure, heat transfer behaviors and reduce pressure loss. The application of the 30° end-trimmed rectangulat winglet placed periodically on the wall of the tested duct is expected to generate a longitudinal vortex flow through the duct to better mixing of flows between the core and the wall resulting in higher heat transfer rate in the duct.

2. Mathematical modeling

The numerical model for fluid flow and heat transfer in the circular tube was developed under the following assumptions: steady three-dimensional, laminar and periodic incompressible fluid flow and ignoring body forces, viscous dissipation and radiation heat transfer. Based on the assumptions, the tube flow is governed by the continuity, the Navier-Stokes equations and the energy equation. In the Cartesian tensor system these equations can be written as follows:
Continuity equation:

$$\frac{\partial}{\partial x_i}(\rho u_i) = 0 \tag{1}$$

Momentum equation:

$$\frac{\partial(\rho u_i u_j)}{\partial x_j} = -\frac{\partial p}{\partial x_i} + \frac{\partial}{\partial x_j}\left[\mu\left(\frac{\partial u_i}{\partial x_j} + \frac{\partial u_j}{\partial x_i}\right)\right] \tag{2}$$

Energy equation:

$$\frac{\partial(\rho u_i T)}{\partial x_i} = \frac{\partial}{\partial x_j}\left(\Gamma \frac{\partial T}{\partial x_j}\right) \tag{3}$$

where Γ is the thermal diffusivity and is given by

$$\Gamma = \frac{\mu}{\mathrm{Pr}} \tag{4}$$

Apart from the energy equation discretized by the QUICK scheme, the governing equations were discretized by the power law differencing scheme, decoupling with the SIMPLE algorithm and solved using a finite volume approach [10]. The solutions were considered to be converged when the normalized residual values were less than 10^{-5} for all variables but less than 10^{-9} only for the energy equation.

Four parameters of interest in the present work are the Reynolds number (*Re)*, friction factor (*f*), Nusselt number (*Nu*) and thermal enhancement factor (*TEF*). The Reynolds number is defined as

$$\mathrm{Re} = \rho \bar{u} D / \mu \tag{5}$$

The friction factor, *f* is computed by pressure drop, Δp across the length of the periodic tube, L as

$$f = \frac{(\Delta p / L)D}{\frac{1}{2}\rho \bar{u}^2} \tag{6}$$

The heat transfer is measured by local Nusselt number which can be written as

$$Nu_x = \frac{h_x D}{k} \tag{7}$$

The average Nusselt number can be obtained by

$$Nu = \frac{1}{A}\int Nu_x \partial A \tag{8}$$

The thermal enhancement factor (*TEF*) is defined as the ratio of the heat transfer coefficient of an augmented surface, *h* to that of a smooth surface, h_0, at an equal pumping power and given by

$$TEF = \left.\frac{h}{h_0}\right|_{pp} = \left.\frac{Nu}{Nu_0}\right|_{pp} = \left(Nu/Nu_0\right)/\left(f/f_0\right)^{1/3} \tag{9}$$

where Nu_0 and f_0 stand for Nusselt number and friction factor for the smooth tube, respectively.

3. Flow configuration

3.1 Winglet geometry and arrangement

The system of interest is a square duct with the 30° end-trimmed rectangulat winglet placed on the square duct wall in tandem with in-line arrangement and pointing upstream as shown in figure 1. The flow under consideration is expected to attain a periodic flow condition in which the velocity field repeats itself from one cell to another. The concept of periodically fully developed flow and its solution procedure has been described in [4]. The air enters the square duct at an inlet temperature, T_{in}, and flows over the 30° end-trimmed rectangulat winglet where *b* is the winglet height, *D* set to 0.05 m, is the square duct diameter and *b*/*H* is known as the blockage ratio, *BR*. The axial pitch, *L* is a distance between the rib cell set to *L* = 2*D* in which *L*/*D* is defined as the pitch ratio, *PR* = 2.0.

To investigate an effect of the interaction between winglet, the winglet blockage ratio, *BR* is varied in a range of *BR* = 0.10 – 0.20 for $\alpha = 30^{\circ}$ and $\beta = 60^{\circ}$ in the current investigation.

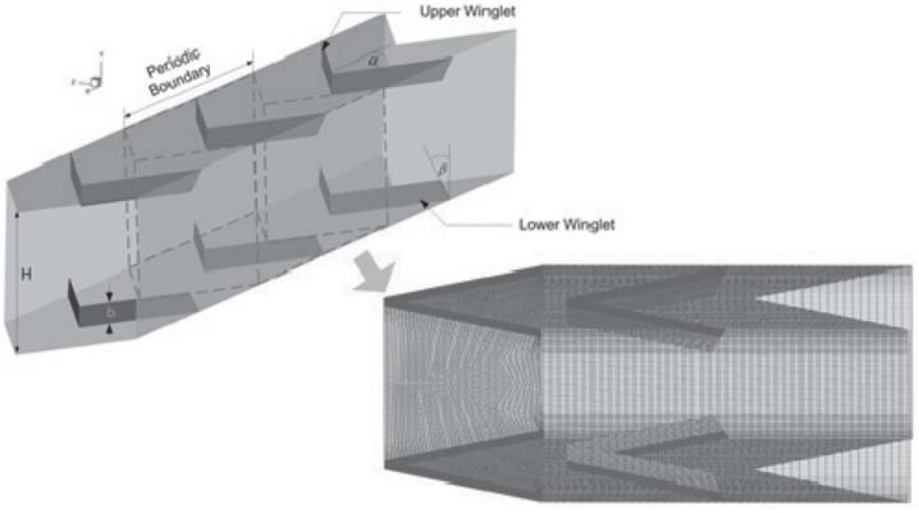

Figure 1 Duct geometry and computational domain of periodic flow

3.2 Boundary conditions

Periodic boundaries are used for the inlet and outlet of the flow domain. Constant mass flow rate of air with 300 K (*Pr*=0.707) is assumed due to periodic flow conditions. The physical properties of the air have been assumed to remain constant at mean bulk temperature. Impermeable boundary and no-slip wall conditions have been implemented over the tube walls as well as the winglet. The constant temperature of the square duct walls is maintained at 310 K while the winglet plate is assumed at adiabatic wall conditions.

3.3 Grid system

The computational domain is resolved by regular Cartesian elements and four grids of 20,600, 42,500, 83,500 and 164,200 cells are used to investigate the grid independence solution. In the test, the variation in *Nu* and *f* values for the 30° end-trimmed rectangulat winglet at *BR*=0.15 and *Re*=800 is marginal (<0.3%) when increasing the number of cells from 83,500 to 164,200, hence the grid system of 83,500 cells was adopted for the current computation.

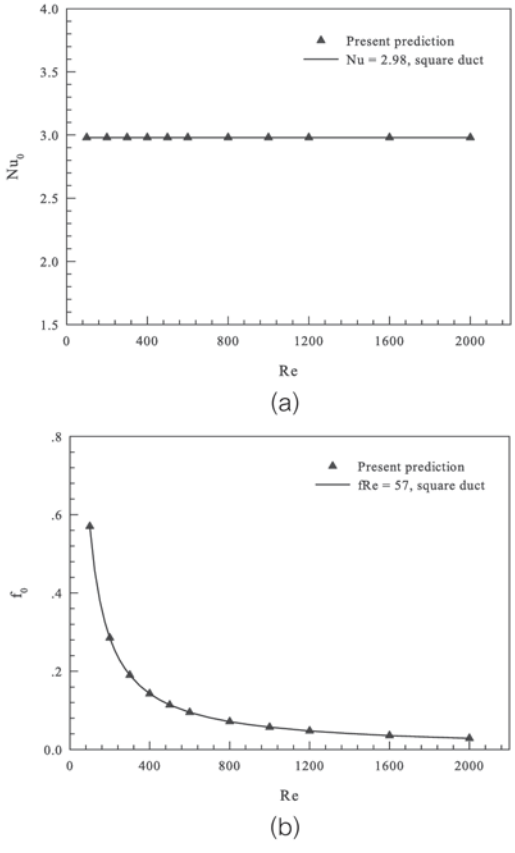

Figure 2 Verification of (a) Nusselt number and (b) friction factor for smooth square duct

3.4 Verification of smooth square duct

Verification of the heat transfer and friction factor of the smooth square duct without winglet is performed by comparing with the previous values under a similar operating condition as shown in figure 2a and 2b, respectively. The present numerical smooth square duct result is found to be in excellent agreement with exact solution values obtained from the open literature [11] for both the Nusselt number and the friction factor, less than ±0.5 % deviation. The exact solutions [11] of the Nusselt number and the friction factor for laminar flows over square duct with constant wall temperature are $Nu_0 = 2.98$ and $f_0 = 57/\mathrm{Re}$, respectively. Therefore, these exact solutions are used to normalize the numerical results of the Nusselt number and the friction factor values.

4. Results and discussion

4.1 Flow structure

The flow and vortex structure in a square duct with 30° end-trimmed rectangulat winglet on the square duct wall can be displayed by considering the streamline and contour plots as depicted in figures 3-5.

Figure 3 show the streamlines in transverse planes at *Re*=800 for the winglet with *BR*=0.15. By considering one module starting from the *WTE* to the next *WTE* with pitch length of 2*L*, there is a main vortex flow through the square duct. For the case of *BR*=0.15, *Re*=800 and *PR*=2 in figure 3, a center of the main vortex flow (or an "eye" of vortex core) at the winglet trailing end (*WTE*) location plane, plane A1, is seen in the region of the downstream winglet cavity near the upstream winglet trailing edge. When moving to the quarter module location (*L*/4), plane A2, a new vortex core center is created in the upstream winglet tip apart from the one, as mentioned in the planes A1 which its size is gradually reduced and vanished. At the half module location (*L*/2), plane A3, the vortex core center appears on the duct sidewall. At the third quarter module location (3*L*/4) as seen in plane A4, a new small vortex core center is generated below the existing one. Then, both appear and the vortex flow repeats itself as it reaches the winglet leading end (*WLE*) of the next module (see plane A5). This vortex flow pattern is similar to the all cases.

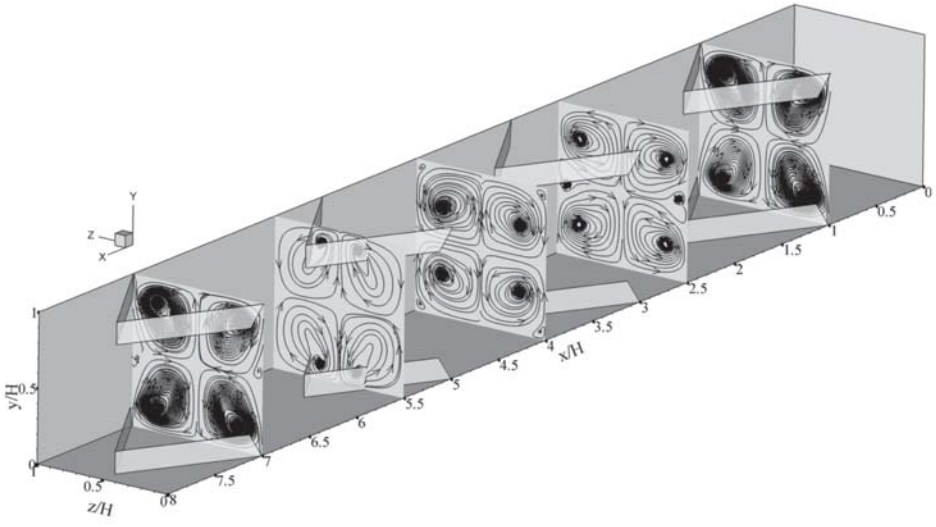

Figure 3 Streamlines in transverse planes for *BR*=0.15 at *Re*=800

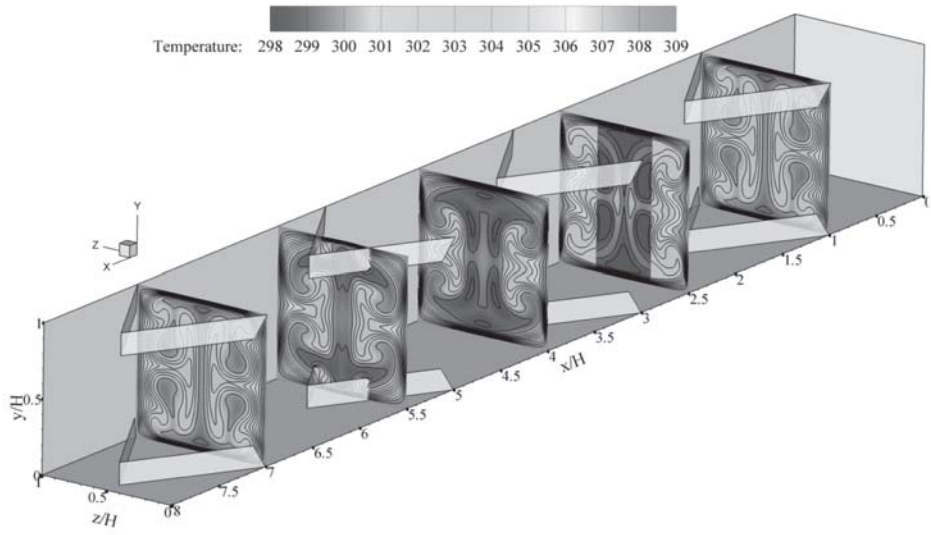

Figure 4 Temperature contours in transverse planes for *BR*=0.15 at *Re*=800

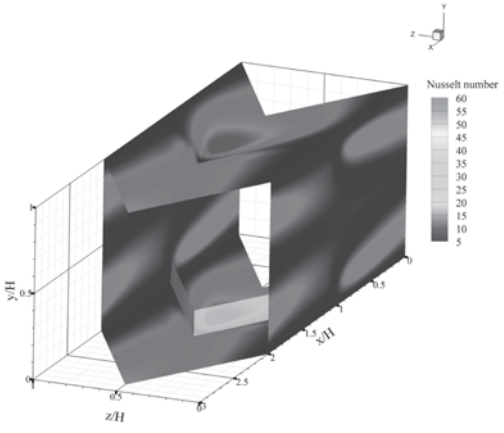

Figure 5 Nu_x Contours for *BR*=0.15 and *Re*=800

4.2 Heat transfer and friction loss

Figure 4 displays the contour plots of temperature field in transverse planes at *Re*=800 for the winglet with *BR*=0.15. The figure shows that there is a major change in the temperature field throughout the square duct. The higher temperature gradient can be observed where the flow impinges the duct walls while the lower one is seen in the region where the temperature is somewhat high indicating that low temperature gradient occurs.

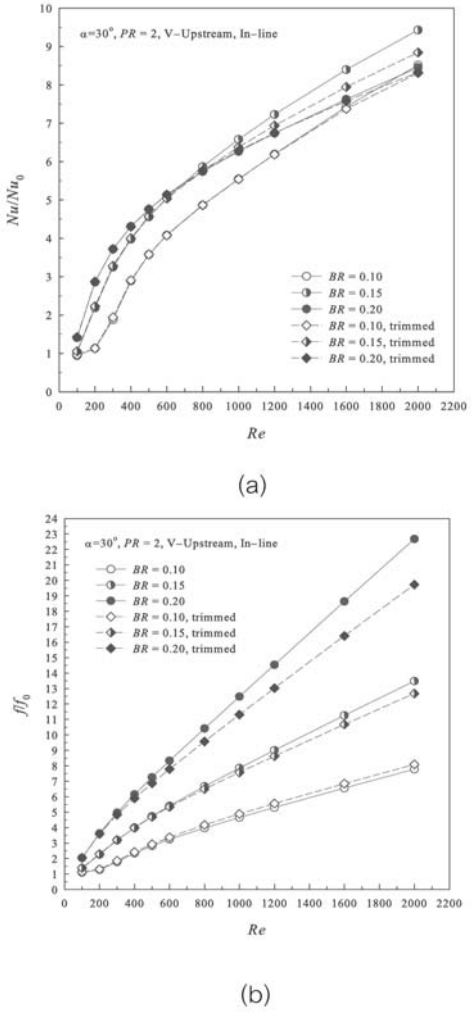

Figure 6 (a) Nu/Nu_0 and (b) f/f_0 versus Reynolds number

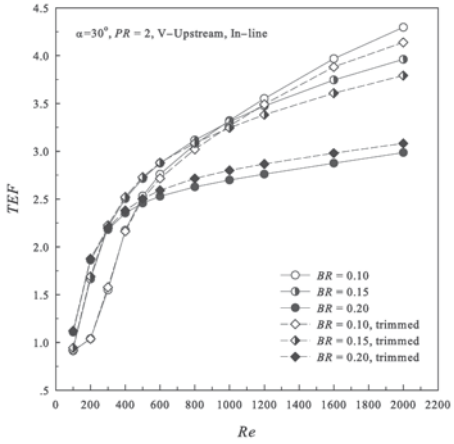

Figure 7 Thermal enhancement factor at various winglet *BR*s

Figure 5 exhibits local *Nu* contours of the square duct wall for the winglet at *Re*=800, *BR*=0.15. It is visible in the figure that a larger area of high *Nu* values can be observed at the upper and lower walls of the module.

The variation of the average Nu/Nu_0 ratio with *Re* for the winglet with various *BR*s and compare with the winglet with no end-trimmed or regular winglet is presented in figure 6a. In the figure, it is visible that the Nu/Nu_0 value tends to increase with the rise of *Re* for all cases. The winglet with *BR*=0.15 provides the highest Nu/Nu_0 value on both end-trimmed and regular winglet. The maximum Nu/Nu_0 values is found to be about 8.70 and 9.50 for *BR*=0.15 in case of end-trimmed winglet and regular winglet, respectively. A closer examination reveals that the use of the end-trimmed winglet with *BR* ranges studied yields average heat transfer rate of about 1.00–8.70 times over the square duct with no end-trimmed winglet, depending on the *BR* values.

Figure 6b displays the variation of the friction factor ratio, f/f_0 with *Re* for various *BR* values and compare with regular winglet. In the figure, it is noted that the f/f_0 tends to increase with the rise of *Re* and *BR* values. The winglet with *BR*=0.20 gives the highest f/f_0 value on both end-trimmed and regular winglet. The friction factor for the end-trimmed winglet and regular winglet appears to be about 1.00-20.00 and 1.00-23.00 times above that for the smooth square duct, respectively. Thus the flow blockage due to the presence of the winglets is a vital factor to cause a high pressure drop in the square duct, the end-trimmed winglet help to decrease pressure loss in comparison with the regular winglet.

5. Conclusions

Numerical computations of laminar periodic flow and heat transfer characteristics in a square duct fitted with 30° end-trimmed rectangular winglet in tandem on the square duct wall with in-line arrangement and pointing upstream are performed. The main vortex flow created by the winglet exists and helps to induce impingement flows over the square duct wall leading to drastic increase in heat transfer in the square duct. The order of heat transfer enhancement is about 1.00-8.70 times for using the end-trimmed rectangular winglet with *BR*=0.10–0.20 at *PR*=2.0. The pressure loss is in a range of 1 to 20 times above the smooth duct. Thermal enhancement factor for the end-trimmed rectangular winglet is higher than unity and its maximum value is about 4.10 at *BR*=0.10 and *PR*=2.00, indicating higher performance over the smooth duct.

6. Acknowledgement

This research was funded by King Mongkut's University of Technology North Bangkok.

7. References

[1] Promvonge P, Thianpong C. Thermal performance assessment of turbulent channel flow over different shape ribs. Int. Commun. Heat Mass Transf., 2008; 35: 1327–1334.

[2] Sripattanapipat S, Promvonge P. Numerical analysis of laminar heat transfer in a channel with diamond-shaped baffles. Int. Commun. Heat Mass Transf., 2009; 36: 32-38.

[3] Han JC, Zhang YM, Lee CP. Augmented heat transfer in square channels with parallel, crossed and V-shaped angled ribs. ASME, J. Heat Transf., 1991; 113: 590-596.

[4] Patankar SV, Liu CH, Sparrow EM, Fully developed flow and heat transfer in ducts having streamwise-periodic variations of cross-sectional area, ASME J. Heat Transf.,1998; 98: 1109-1151.

[5] Berner C, Durst F, McEligot DM, Flow around baffles, ASME J. Heat Transf., 1984; 106: 743-749.

[6] Lopez JR, Anand NK, Fletcher LS, Heat transfer in a three-dimensional channel with baffles. Numer. Heat Transfer. Part A: Appl.,1996; 30: 189-205.

[7] Promvonge P, Sripattanapipat S., Tamna S, Kwankaomeng S, Thianpong C, Numerical investigation of laminar heat transfer in a square channel with 45 deg inclined baffles. Int. Commun. Heat Mass Transf., 2010; 37: 170-177.

[8] Promvonge P, Sripattanapipat S, Kwankaomeng S, Laminar periodic flow and heat transfer in square channel with 45° inline baffles on two opposite. Int. J. Therm. Sci., 2010; 49: 963-945.

[9] Murata A, Mochizuki S, Comparison between laminar and turbulent heat transfer in a stationary square duct with transverse or angled rib turbulators. Int. J. Heat Mass Transf., 2001; 44: 1127-1141

[10] Patankar SV, Numerical heat transfer and fluid flow, McGraw-Hill. New York; 1980.

[11] Incropera F, Dewitt PD. Introduction to heat transfer. 5th ed, John Wiley & Sons Inc; 2006.

8. Nomenclature

A	channel wall area, m^2
BR	blockage ratio, (b/H)
WLE	winglet leading edge
WTE	winglet trailing edge
b	winglet height, m
D_h	duct hydraulic diameter, (=2HW/(H+W))
f	friction factor
H	duct height, m
h	heat transfer coefficient, W m^{-2} K^{-1}
k	thermal conductivity, W m^{-1} K^{-1}
L	cyclic length of one module, m
Nu	Nusselt number, hD/k
Pr	Prandtl number
PR	pitch or spacing ratio, L/H
Re	Reynolds number, $\rho \overline{u}\, D/\mu$
T	temperature, K
u_i	velocity in x_i-direction, m s^{-1}
$\overline{u}$	mean velocity in channel, m s^{-1}
W	duct width (H), m

Greek letter

μ	dynamic viscosity, kg $s^{-1}m^{-1}$
Γ	thermal diffusivity
α	orifice angle of attack, degree
η	thermal enhancement factor
ρ	density, kg m^{-3}

Subscript

0	smooth duct
w	wall
pp	pumping power